1.0

2.8   2.5

3.2   2.2

3.6

4.0   2.0

1.1

1.8

1.25   1.4   1.6

MICROCOPY RESOLUTION TEST CHART
NATIONAL BUREAU OF STANDARDS-1963

(12)

Tokamak Plasma Heating with Intense Pulsed Ion Beams
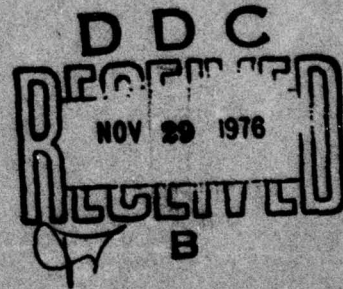
EDWARD OTT

Dept. of Electrical Engineering
Cornell University
Ithaca, New York 14853

and

WALLACE M. MANHEIMER

Plasma Dynamics Branch
Plasma Physics Division

October 1976

D D C

NOV 29 1976

B

NAVAL RESEARCH LABORATORY
Washington, D.C.

REPORT DOCUMENTATION PAGE		READ INSTRUCTIONS BEFORE COMPLETING FORM
1. REPORT NUMBER NRL Memorandum Report 3394	2. GOVT ACCESSION NO.	3. RECIPIENT'S CATALOG NUMBER
4. TITLE (and Subtitle) TOKAMAK PLASMA HEATING WITH INTENSE PULSED ION BEAMS		5. TYPE OF REPORT & PERIOD COVERED Interim report on a continuing NRL problem.
		6. PERFORMING ORG. REPORT NUMBER
7. AUTHOR(s) Edward Ott, and Wallace M. Manheimer		8. CONTRACT OR GRANT NUMBER(s) NRL-MR-3394
9. PERFORMING ORGANIZATION NAME AND ADDRESS Naval Research Laboratory Washington, D.C. 20375		10. PROGRAM ELEMENT, PROJECT, TASK AREA & WORK UNIT NUMBERS NRL Problem H02-37 AEC-AT(49-20)
11. CONTROLLING OFFICE NAME AND ADDRESS Energy Research and Development Administration Washington, D.C. 20545		12. REPORT DATE October 1976
		13. NUMBER OF PAGES 36
14. MONITORING AGENCY NAME & ADDRESS(if different from Controlling Office)		15. SECURITY CLASS. (of this report) UNCLASSIFIED
36 p.		15a. DECLASSIFICATION/DOWNGRADING SCHEDULE

16. DISTRIBUTION STATEMENT (of this Report)

Approved for public release; distribution unlimited.

17. DISTRIBUTION STATEMENT (of the abstract entered in Block 20, if different from Report)

18. SUPPLEMENTARY NOTES

19. KEY WORDS (Continue on reverse side if necessary and identify by block number)

Tokamak
Ion beam
Plasma heating

20. ABSTRACT (Continue on reverse side if necessary and identify by block number)

The recent availability of intense, space-charge-neutralized, energetic ion beams has led us to explore the possibility of using them for heating tokamak plasmas. The following key problems for this application are investigated: (i) beam injection perpendicular to $\underline{B}$, (ii) beam propagation across $\underline{B}$ in vacuum, and (iii) cross-field beam propagation and energy deposition in plasma. It appears possible that, for proper values of the beam energy, radius and current, an intense ion beam can penetrate to the interior of a tokamak plasma and deposit its energy there.

DD FORM 1473 EDITION OF 1 NOV 65 IS OBSOLETE
1 JAN 73

i

251 950

REPORT DOCUMENTATION PAGE

NRL Memorandum Report 3584

CORONAL PLASMA HEATING WITH INTENSE
PULSED ION BEAMS

Naval Research Laboratory
Washington, D.C. 20375

Energy Research and Development Administration
Washington, D.C. 20545

UNCLASSIFIED

KEY WORDS

The recent availability of intense space-charge-neutralized, medium-atomic-number ion beams has led us to explore the possibility of using them for heating toroidal plasmas. The following two mechanisms for this application are investigated: (i) beam injection perpendicular to B-field lines, and (ii) beam injection, and (iii) combined beam propagation and heating limited to plasmas. It appears possible that, for power flux of the beam into the plasma...

CONTENTS

iii

TOKAMAK PLASMA HEATING WITH INTENSE PULSED ION BEAMS

I. INTRODUCTION

Recently, sources of very intense ion beams have become available. Experimental advances,[1,2] as well as theoretical understanding[3-6] of the production of such beams, continue to proceed rapidly. The availability of these beams naturally leads to the proposal of uses to which they may be put. Several such suggestions have recently been advanced.[7] In this paper we propose and evaluate the use of intense ion beams for tokamak heating.

Similar proposals have been made for intense electron beams, but the problem of transporting an electron beam from an external injection point across magnetic surfaces to the plasma interior appears to be difficult (cf. Ref. 8 for progress on this topic).

Intense ion beams can actually be charge neutralized after they are produced by dragging along an equal number of electrons. (In this mode it is possibly more accurate to talk of an intense "plasma beam", but we shall stick to the term ion beam because of the way the beam is produced.) As is well-known,[9-11] such a neutralized group of ions and electrons can move across a vacuum magnetic field, essentially unimpeded, if $(\omega_{pi}/\Omega_i)^2 \gg 1$ (ω_{pi} and Ω_i are the ion plasma and gyro frequencies in the beam), by setting up surface polarization charges in such a way that the electric field in the beam is $- \underset{\sim}{V} \times \underset{\sim}{B}$. This has been verified experimentally[10,11] in a number of studies with plasma guns and laser produced plasmas. Thus the propagation

Note: Manuscript submitted September 30, 1976.

1

of an ion beam from an external beam production point to the edge
of a plasma may be possible, although, as we shall
see later, there are some important complicating effects which alter
this simple picture. The propagation of the beam across a magnetic
field in a plasma and the deposition of beam energy in the plasma
presents a more complex problem, whose solution is of great importance
for the application proposed here.

The organization of the rest of this paper is as follows. In
Sections II and III we discuss the production and extraction of ion
beams. In Section IV we study beam propagation across a magnetic
field in a vacuum. It is shown that the polarization fields, in
addition to allowing beam transport across $\underset{\sim}{B}$, also cause the beam to
expand along $\underset{\sim}{B}$. A simple criterion for such beam spreading to be
important is given. Section V discusses cross-field propagation
and energy deposition in a plasma. In Section VI we consider the use
of intense ion beams for plasma heating in tokamaks.

II. BEAM PRODUCTION

The simplest conception of an ion diode accelerator is a planar anode-cathode gap in which the anode and cathode are capable of emitting ions and electrons respectively. Solution of this problem for space charge limited flow[12] shows that the ratio of ion to electron current density is $(j_i/j_e) = 1.85 (Zm_e/m_i)^{\frac{1}{2}}$. Since the electrons and ions both fall through the same potential energy difference, this is also the ratio of power delivered to the ion beam to power delivered to the electron beam. Thus most of the energy goes to electrons, and the ion energy efficiency is low. The basic problem is thus to prevent energy from being given to electrons so that the energy delivered to the gap goes to producing the ion beam. Recently, two methods of accomplishing this have been demonstrated: (1) the reflex triode,[1,3-5] and (2) the magnetically insulated ion diode.[2,3,6]

A schematic illustration of a reflex triode is shown in Fig. 1. Two cathodes are located at $x = \pm L$ on either side of an anode at $x = 0$. The anode material and construction are such that electrons easily pass through it. Assuming perfect transmission, electrons would simply be emitted from one cathode and collected at the other with zero velocity. Thus no energy would be given to the electrons. Ions are extracted from both sides of the anode surface and pass through the two cathodes, as shown in Fig. 1. In practice, the anode is not completely transparent to electrons (e.g. electron scattering in the anode will lead to a distribution of electrons trapped in the

3

gap potential well[13]), and this allows   increased ion currents as well as a small electron current collected at the anode. Nevertheless, ion energy efficiencies[14] in excess of 60% have been achieved (for both beams). Currently ion beams energies $\gtrsim$ 1 MV. and currents $\sim$ 1 kA/cm^2 have been produced.   It is to be expected that much higher energies and currents will be reported in the near future. One disadvantage of the reflex triode is that two beams propagating in opposite directions are produced. Thus one must find a way of simultaneously utilizing both beams (or else settle for one half of the possible energy efficiency). Various schemes for injecting both beams are possible, but will not be discussed here.

Figure 2 illustrates a magnetically insulated ion diode. The basic idea is that a magnetic field of the proper strength is applied parallel to the anode and cathode surfaces and prevents the flow of electrons across the gap but is not strong enough to prevent ion flow. Roughly speaking, the ion Larmor radius (based on the ion velocity in falling through the applied gap voltage) exceeds d, the gap spacing, but the same quantity for electrons is less than d. (Of course there is some modification of the above statement due to self-consistent electron and ion charge and current density within the gap [cf. Ref. 3].)

Related to the simple picture of magnetically insulated ion diodes in Fig. 2 is the recent discovery[15] that pinched electron diodes (cf. Fig. 3) can have high ion efficiencies. Here the magnetic insulation is from magnetic fields that arise naturally rather than

4

from externally applied magnetic fields. The magnetic field created by the current in the diode tightly pinches the electrons to the axis but does not influence the more massive ions. In this way the ion beam to electron beam current ratio is greatly enhanced, especially for large aspect ratio diodes (i.e. R/d in Fig. 3 large).[16]

If one considers an anode-cathode gap with applied voltage V megavolts, then, according to the Langmuir-Child law, the ion current density produced (in amperes/cm^2) is

$$j_{LC} \cong 60 \; V^{3/2}/d^2 \;\;,$$ (1)

(where d is in centimeters) if it is assumed that no electrons are present. In actual fact, the presence of electrons in the gap allows the possibility that the space charge limited ion current can be enhanced by a factor $\alpha (\alpha \equiv j_i/j_{LC})$. For example, reflex triode operation with enhancements as large as $\sim 10^2$ has been observed.[14]

Finally we note a limitation on the current pulse time. Generally, plasma is formed on the anode and cathode surfaces. In the absence of a magnetic field these plasmas expand toward each other. This results in shorting out the gap (called "gap closure") at a time

$$t_c \cong d/(v_a + v_c)$$ (2)

5

where v_a and v_c are the anode and cathode plasma velocities. For example,[17] values of $t_c \sim 40$ nanosec have been measured for $d = 0.34$cm. Application of a magnetic field transverse to the gap has been observed[17] to have the beneficial effect of greatly increasing t_c so that longer current pulses would be possible (e.g. in magnetically insulated diodes).

III. BEAM INJECTION

As an example of how an ion beam can be injected into a tokamak, consider the situation shown in Fig. 4. A reflex triode is situated in a guide tube which leads into the side wall of a tokamak. The triode and the guide tube are subjected to a longitudinal guide field which curves to merge with the main tokamak magnetic field. The ion beam emerging from the right side of the triode is neutralized by electrons dragged off plasma on the outside surface of the cathode. Thus a neutralized beam will propagate down the drift tube. As the beam reaches the end of the guide tube, the field lines curve to eventually be at right angles to the initial beam velocity. This problem is similar to that of plasma motion along a curved magnetic field analyzed years ago by Schmidt.[9] Schmidt demonstrated that for $\omega_{pi}^2 \gg \Omega_i^2$ a polarization field will be set up by charge separation within the beam due to adiabatic guiding center inertial drifts,

$$\underset{\sim}{E}_o \cong -\underset{\sim}{V}_o \times \underset{\sim}{B}$$

where $\underset{\sim}{V}_o$ is the beam velocity _in the guide tube_. The quantity $\underset{\sim}{E}_o$ is actually slightly less than $- \underset{\sim}{V}_o \times \underset{\sim}{B}$ by an amount of order Ω_i^2/ω_{pi}^2. Thus the beam moves essentially unimpeded by the magnetic field.

In order for the above considerations to be valid the beam density must be sufficiently large that $\omega_{pi}^2 \gg \Omega_i^2$. From the Langmuir-Child law the beam density is

7

$$n = 3 \times 10^{11} \, \alpha \, V/d^2 (cm^{-3}) \qquad (3)$$

where V is in MV and d in cm, and we have included the enhancement factor α introduced in Sec. II. n can be further increased by converging the $\underline{B}$ - field in the guide tube. As will be evident from the example treated in Sec. VI, the condition $\omega_{pi}^2 \gg \Omega_i^2$ can be easily achieved.

One could equally well use a pinched electron diode[15] in Fig. 4. The applied longitudinal field could be small compared to the self-consistent pinch field in the diode, thus leaving the diode characteristics uneffected. On the other hand, the pinch field exists for only a short time and so does not diffuse through the conducting electrodes. Thus, once the ion beam emerges from the right side of the cathode it is in the purely longitudinal applied field and is not effected by the pinch field.

It is less obvious how to inject a neutralized beam to travel perpendicular to the applied tokamak field, if a magnetically insulated ion diode (Fig. 2) is to be used. The problem is that the applied insulating field will exist on both sides of the cathode (it will probably be in existence long compared to the $\underline{B}$ - field diffusion time through the cathode) and will prevent electrons from being dragged off the side of the cathode as the ion beam emerges. Thus the emergent ions are unneutralized and will only propagate a distance of the order of their Larmor radius, a distance too short to be of interest in this application. It may be possible to get around this limitation, but it appears to be difficult.

8

IV. PROPAGATION OF THE BEAM IN VACUUM

As was shown in the previous section, when the ion beam passes from the guide pipe into the tokamak in which it propagates perpendicular to $\underset{\sim}{B}$, a polarization electric field is set up which gives the necessary $\underset{\sim}{E} \times \underset{\sim}{B}$ drift. Due to the cylindrical geometry, outside the beam, this polarization field has a component parallel to $\underset{\sim}{B}$. This leads to forces on the beam such that the beam tends to expand along the magnetic field. As it expands, the density decreases so propagation becomes more difficult. This expansion along the field appears to be the dominant effect which limits the distance the beam can propagate in the vacuum. This effect is demonstrated below.

In the reference frame moving with the initial beam velocity, $\underset{\sim}{V}_o$, the beam acts like a dielectric with dielectric constant $\epsilon = \epsilon_o (1 + \omega_{pi}^2 / \Omega_i^2)$. We assume that the beam is initially of circular cross-section with radius $r = a$. Thus once the beam enters the tokamak and is propagating (along y, say) perpendicular to the main magnetic field, $\underset{\sim}{B} = B\underset{\sim}{z}_o$, the induced electric field can be found by transferring to a frame moving with $\underset{\sim}{V}_o$. In this frame we solve Laplace's equation in the plane perpendicular to the beam velocity, $\nabla^2 \phi = 0$, using cylindrical coordinates (r, θ) where θ is the angle to the x axis. The boundary conditions at the beam edge and the condition at infinity are continuity of ϕ and $\epsilon \partial \phi / \partial r$ at $r = a$ ($\epsilon = \epsilon_o$ for $r > a$ and $\epsilon = \epsilon_o [1 + (\omega_{pi}/\Omega_i)^2]$ for $r < a$) and $\phi \to - E_o x$ at $r \to \infty$, where $E_o = V_o B$. We find that the induced z-component of electric field outside the beam is

$$E_z = (a/r)^2 E_o \sin 2\theta [1 + (\Omega_i/\omega_{pi})^2]^{-1} \qquad (4a)$$

and the electric field in the beam is constant and purely in the x-direction,

$$\underset{\sim}{E} = \underset{\sim}{x}_o 2E_o/[2 + (\omega_{pi}/\Omega_i)^2]. \qquad (4b)$$

The polarization surface charge density at $r = a$ can be calculated from the difference between the normal fields inside and outside the beam. The result is

$$\rho_s(\theta) = 2\epsilon_o \frac{\omega_{pi}^2}{\omega_{pi}^2 + 2\Omega_{ci}^2} E_o \cos\theta \qquad (5)$$

From the surface charge density, the force per unit area in the z direction can be calculated from $F_z(\theta) = E_z(r = a^+) \rho_s(\theta)$ to be

$$F_z(\theta) = 2\epsilon_o \left(\frac{\omega_{pi}^2 E_o}{\omega_{pi}^2 + 2\Omega_{ci}^2} \right) \sin\theta \cos^2\theta \qquad (6)$$

Note that F_z is directed outward from the beam, $F_z(\theta) > 0$ for $\pi > \theta > 0$ and $F_z(\theta) < 0$ for $2\pi > \theta > \pi$.

The way in which the beam will expand along the field line due to the presence of this force is not at all obvious. Probably the electron polarization charge layer will initially expand much

10

faster than the ions in the positive charge layer. The electrons will only be arrested when sufficient positive charge is left behind to reverse the sign of the parallel force. The electron sheath may expand along a field line for a distance comparable to the radius of the beam so that the charge layer may become grossly distorted.

As a very crude approximation, we will say that the beam expands outward retaining an elliptical shape of major radius b and minor radius a equal to the initial radius. Then, integrating Eq. (6) (assuming $\omega_{pi}^2 \gg \Omega_{ci}^2$) over θ to determine the total outward force, we find an approximate equation for b

$$\frac{d^2}{dt^2} \frac{b}{2} n_o M \frac{\pi a^2}{2} = \frac{4}{3} a \epsilon_o E_o^2 , \qquad (7)$$

where n_o is the initial beam density. From (7) a rough expression for the time for the beam to expand along z by its own radius is then given by

$$\tau_E \sim \frac{\omega_{pi}}{\Omega_{ci}} \frac{a}{V} . \qquad (8)$$

While the beam propagates forward at speed V, the positive and negative sheaths on the top and bottom only propagate forward at about V/2 since the electric field is reduced to approximately zero at the outer edge of the sheaths.[9] Thus the sheaths are constantly falling behind the beam and are being replenished from the interior.

11

From the expression for the surface charge density, we find that
the thickness of the sheath is given by

$$\Delta_s \approx \frac{2\epsilon_o}{ne} VB \cos \theta . \tag{9}$$

If the sheath falls behind at a velocity $V/2$, one can calculate that
the time for the beam to lose half its particles due to sheath loss
is given roughly by

$$\tau_s = \frac{\omega_{pi}}{\Omega_{ci}} \frac{a}{V} \omega_{pi} \tau_b \tag{10}$$

where τ_b is the time duration of the beam pulse. Clearly, since
$\omega_{pi} \tau_b \gg 1$ for cases of practical interest, we see that $\tau_s \gg \tau_E$
so that expansion along the field lines is the dominant effect limiting
the propagation of the beam in vacuum.

Another possible physical effect which can stop the beam propagation
in the vacuum is short circuiting along a field line. That is, if the
same magnetic field line passes through both the positive and negative
polarization charge layer, current can flow along the field line and
short circuit the charge separation. However, as was pointed out in
similar work on octupoles,[10] the distance along the field line between
the positive and negative charge layers must be short (not much longer
than the radius of the beam) in order for this to happen. This is
quite reasonable intuitively. If an electron, after leaving the charge

12

layer, has traveled a long distance and has not reached the positive
layer, it leaves behind positive charge which will pull it back along
the field line.

For example, in a tokamak the magnetic field lines fill nested
magnetic surfaces so that an electron traveling along a field line
which passes through the negative charge layer will ultimately pass
through the positive charge layer; and hence it might be thought that
the field could be shorted out. This consideration, however, is
irrelevant not only because the distance an electron must travel is
much longer than a beam radius, but also because $2\pi R/c$ is typically
longer than the duration of the beam !

V. PROPAGATION AND ENERGY DEPOSITION IN THE PLASMA

After the beam has propagated from the wall through the vacuum region of the tokamak, it enters the plasma. We now discuss qualitatively how the beam can propagate and deposit its energy. To begin, assume a two dimensional picture with no variation along $\underline{B}$. Since $\omega_{pi}^2 \gg \Omega_i^2$, the electric field in the beam must be small in the frame moving with the initial beam velocity, $\underline{V}_o$, (the beam acts like a perfect conductor) so that the surface of the beam is approximately an equipotential. Since the plasma, when it $\underline{E} \times \underline{B}$ drifts remains along equipotentials, the plasma does not interpenetrate the beam but rather is pushed out of its way. Such a two dimensional flow pattern in the frame moving with the beam is shown in Fig. 5 in the plane perpendicular to $\underline{B}$. Of course the geometry is not two dimensional, but cylindrical. Each magnetic field line in the beam must be at a different potential in order to maintain the polarization electric field which convects the beam. However the potential of the background plasma is the same on different field lines. Therefore the background plasma attempts to short circuit the polarization field and stop the beam at the outside of the tokamak plasma, rather than the center. At the present time the dynamics of the short circuiting process is not clear to us. However, even if short circuiting occurs a sufficiently intense beam will propagate through the plasma. To see this imagine that the polarization field is completely shorted out so that the forward motion of the beam is converted to cyclotron motion. Then the diamagnetic current on the beam surface can exclude the tokamak magnetic field as long as the tokamak magnetic field energy density is smaller than the beam energy density, or that the (unneutralized) beam

14

current is large enough to give field exclusion. One can easily show
that this reduces to

$$V_o/V_A > 1, \tag{11}$$

where V_A is the Alfven speed in the beam. If Eq. (11) is satisfied,
the beam will exclude the magnetic field as shown in Fig. 6 and
penetrate the plasma. In order to show the existence of such a mode
of beam propagation with magnetic field exclusion in the beam interior,
the Appendix demonstrates a self-consistent beam equilibrium with the
above properties.

Such a flow pattern shown in Figs. 5 and 6 is unstable to the
Kelvin-Helmholtz instability as long as the beam velocity is less than
$2\sqrt{2}\ V_A$ where V_A is the Alfven speed.[18] [This is analogous to the result
for the ion-ion instability[19] where the plasma and beam do interpenetrate.
There the beam velocity must be less than twice the Alfven speed for
instability to be possible.] As long a $V \lesssim 2V_A$, the spacial growth
length of the Kelvin-Helmholtz instability is given by[18]

$$L_{KH}^{-1} \sim k\ \frac{(\rho_p \rho_p)^{\frac{1}{2}}}{\rho_b + \rho_p} \tag{12}$$

where ρ_b and ρ_p are the mass densities of the beam and plasma respec-
tively. Assuming that the wave number which gives most effective
mixing is $k \cong a^{-1}$, we find $L_{KH} \sim a(\rho_b + \rho_p)/(\rho_b \rho_p)^{\frac{1}{2}}$. Assuming that
about five growth lengths are needed to mix the beam and plasma, one
can choose the beam radius and density so that

15

$$a^{-1} \int_0^{r_o} dr [\rho_b \rho_p(r)]^{\frac{1}{2}} / [\rho_b + \rho_p(r)] \cong 5 , \qquad (13)$$

where r_o is the radius of the plasma. This is an approximate condition
for the beam to propagate to the plasma interior and deposit its
energy there. If the beam and central plasma densities are equal,
then from (13) the beam radius should be about one tenth of the plasma
radius, where we assume a plasma density profile of the form
$\rho_p(r) = \rho_p(o) [1 - (r/r_o)^2]$.

16

VI. TOKAMAK HEATING: AN EXAMPLE

We now discuss the problem of heating a reactor[20] to a temperature of 10 kev with intense ion beams. Assuming a pulse time τ, the total energy of the beam pulse is

$$E_b = VI\tau = 2 \times 10^{-10} \pi a^2 V^{3/2} \tau n_o$$

in Megajoules. If the tokamak has major radius R and the plasma has radius r_p (both in cm), and average density $\bar{n}$ (in cm^{-3}), then the energy in Megajoules to heat the electrons and ions to a temperature of 10 kev is

$$\epsilon_p = 6.4 \times 10^{-21} \bar{n} \pi^2 r_p^2 R.$$

Taking a voltage of 5 Megavolt, $(r_p/a) = 10$, $\bar{n}/n_o = 0.5$ and $\tau = 3 \times 10^{-8}$ sec, we find that about ten pulses are needed for a reactor with a radius of 5 meters. If the central plasma (and beam) density is $5 \times 10^{13} cm^{-3}$, and the magnetic field is 5×10^4 Gauss, then Eqs. (11) and (13) are satisfied, and $V < 2\sqrt{2} V_A$. Thus the beam should deposit its energy near the center of the plasma. Using Eq. (3) we obtain for this example $d \overset{\sim}{\lesssim} 0.1 \, \alpha^{\frac{1}{2}} cm$. Finally, let us note that for ion beam heating of tokamaks there are many possible parameters to vary including beam voltage, current, pulse time, beam radius and injection angle. This flexibility increases the likelihood that parameters can be found for which the beam will propagate to the center of the plasma and deposit its energy there.

REFERENCES

1. S. Humphries, J. J. Lee and R. N. Sudan, Appl. Phys. Lett. 25, 20 (1974); S. Humphries, J. J. Lee and R. N. Sudan, J. Appl. Phys. 46, 187 (1975); S. Humphries, R. N. Sudan and W. C. Condit, Appl. Phys. Lett. 26, 667 (1975); C. A. Kapetanakos, J. Golden and F. C. Young, Nucl. Fusion, 16 (1976); J. Golden, C. A. Kapetanakos, R. Lee and S. Goldstein, Proceedings of the International Conference on Electron Beam Research and Technology, Albuquerque, New Mexico, U.S.A., Nov. 1975; D. Prono and J. W. Shearer, ibid; M. Di Capna, R. Huff and J. Creedon, ibid.

2. P. Dreike, C. Eichenberger, S. Humphries and R. N. Sudan, J. Appl. Phys. 47, 85 (1976); H. H. Fleischmann and S. C. Luckhardt, Bull. Am. Phys. Soc. 20, 1380 (1975).

3. T. M. Antonsen and E. Ott, Phys. Fluids 19, 52 (1976).

4. T. M. Antonsen and E. Ott, Appl. Phys. Lett. 28, 424 (1976).

5. R. Huff and I. Smith, Bull. Am. Phys. Soc. 14, 870 (1974); T. M. Antonsen and E. Ott, ibid. p. 871; J. M. Creedon, I. D. Smith and S. D. Prono, Phys. Rev. Lett. 35, 91 (1975).

6. R. Lovelace and R. N. Sudan, Phys. Rev. Lett. 31, 1174 (1973); K. D. Bergeron, Bull. Am. Phys. Soc. 14, 1381 (1975); R. Lovelace and E. Ott, Phys. Fluids 17, 1263 (1974); E. Ott and R. Lovelace, Appl. Phys. Lett. 7, 378 (1975); F. Winberberg, Physics of High Energy Density (Academic Press, New York, 1971), p. 370; N. Rostoker, IEEE Trans. Nucl. Sci. NS-19, 301 (1972).

7. R. N. Sudan and E. Ott, Phys. Rev. Lett. 33, 355 (1974); H. H.

Fleischmann, and T. Kammesh, Nucl. Fusion 15, 1143 (1976);

F. Winterberg, Plasma Phys. 17, 69 (1975); M. J. Clauser, Phys.

Rev. Lett. 35, 848 (1975); E. Ott and R. N. Sudan, Appl. Phys.

Lett. 29, 5 (1976); S. Humphries, Plasma Phys. 18, (1976).

8. D. F. Brower, B. R. Kusse and G. D. Meixel, IEEE Trans. PS-2,
    193 (1974); J. Benford, B. Ecker and V. Bailey, Phys. Rev. Lett.
    33, 574 (1974).

9. G. Schmidt, Phys. Fluids 3, 961 (1960).

10. R. A. Dory, et al., Phys. Fluids 9, 997 (1966).

11. I. I. Demidenko et al., Zh. Tekh. Fiz. 36, 1819 (1966); T. Matoba
    and S. Ariga, J. Phys. Soc. Jap. 30, 1477 (1971); V. G. Zykov et
    al., Zh. Tekh. Fiz. 34, 1094 (1964); I. I. Demidenko et al., Zh.
    Tekh. Fiz. 34, 1183 (1964); G. O. Barnet, Phys. Fluids 12, 2492
    (1969); D. A. Baker and J. E. Hammel, Phys. Fluids 8, 713 (1965).

12. I. Langmuir, Phys. Rev. 33, 955 (1929).

13. Antonsen and Ott[4] have given a self-consistent solution including
    the actual distribution function resulting from electron scattering
    in the anode.

14. C. A. Kapetanakos (private communication).

15. S. A. Goldstein and R. Lee, Phys. Rev. Lett. 35, 1079 (1975);
    J. W. Poukey et al., Phys. Rev. Lett. 35, 1806 (1975); J. W.
    Poukey in Proceedings of the Thirteenth Symposium on Electron,
    Ion, and Photon Beam Technology, Colorado Springs, Colorado (1975);
    A. E. Blaugrund, G. Cooperstein and J. R. Boller, Bull. Am. Phys.
    Soc. 20, 1252 (1975).

16. Goldstein and Lee[15] have shown that $(I_1/I_e) > (R/d)(Zm_e/m_1)^{\frac{1}{2}}$ in pinched diodes.

17. T. J. Orzechowski and G. Bekefi, Phys. Fluids 19, 43 (1976).

18. J. A. Fejer, Phys. Fluids 7, 499 (1964).

19. K. Papadopoulos et al., Phys. Fluids 14, 849 (1971).

20. W. M. Manheimer, E. Ott and I. Haber, Proceedings of the Third International Meeting on Theoretical and Experimental Aspects of Heating of Toroidal Plasmas, Grenoble, France, June 28 to July 2, 1976.

APPENDIX: Equilibria for Cross Field Beam Propagation in Plasma

In this appendix we will show that it is possible to produce a magnetically shielded region through which the beam can propagate. Our interpretation is that the head of the beam meets the plasma at one point and stops. In stopping, it sets up a diamagnetic current which cancels the ambient tokamak field, allowing the rest of the beam to propagate through. Thus the beam front is continuously peeled off, creating a field free region behind it through which the remainder of the beam propagates.

For simplicity, consider a two dimensional situation in the (x,y) plane perpendicular to $B(y)\underline{z}_o$, with the beam propagating in x. Since background plasma is assumed to short out any electric fields, we set $\underline{E} \equiv 0$ in the laboratory frame. The beam ions are assumed to satisfy the Vlasov equation so that the beam ion distribution function depends only on constants of the motion, $F_i = F_i(v_\perp^2, v_z, P_x)$ where $v_\perp^2 = v_x^2 + v_y^2$, $P_x = m_i v_x - eA(y)$, and $B(y) \equiv dA/dy$. Since the electrons are much less massive we use the fluid equations. From the y - component of the beam electron momentum equation we have $-dp_e/dy - J_e\, dA/dy = 0$ or $J_e = -dp_e/dA$, where J_e is the beam electron current (which is in the x direction) and p_e is the electron pressure. Now using the $\nabla \times \underline{B}$ Maxwell equation we have

$$\frac{d^2A}{dy^2} = \mu_o \left[J_i(A) - \frac{dp_e}{dA} \right] \quad , \tag{A1}$$

21

where

$$J_i(A) = e \int v_x F_i \, d^3v,$$

which can be written $J_i(A) = - \, dp_i/dA$, after using a parts integration, where the yy beam ion pressure is

$$p_i(A) = m_i \int v_y^2 F_i \, d^3v.$$

Now multiplying Eq. (A1) by dA/dy and integrating over y we obtain

$$\frac{1}{2\mu_o} \left(\frac{dA}{dy}\right)^2 + p_e(A) + p_i(A) = \frac{1}{2\mu_o} B_o^2, \qquad (A2)$$

where p_e and p_i go to zero away from the beam, B_o is the external magnetic field outside the beam. Equation (A2) is, of course, just the y-component of the total pressure equation.

We now demonstrate how a magnetically shielded equilibrium can be formed. It seems reasonable to assume that the beam electron random velocity is roughly the same as the beam ion random velocity, thus the electron pressure is much less than the ion pressure. We will begin by neglecting the electron pressure. However, as we will shortly see, a small electron pressure is necessary for the formation of the magnetically shielded equilibrium.

For concreteness, let us pick an ion distribution function:

$$F_i = N_o \delta(v_\perp - v_{\perp o}) \delta(v_x - \frac{e}{M} A) \delta(v_z). \qquad (A3)$$

22

Then if electron pressure is neglected, Eq. (A2) reduces to

$$\frac{1}{2} \left(\frac{dA}{dy}\right)^2 + \mu_o N M v_{\perp o}^2 \left(1 - \left(\frac{eA}{M v_{\perp o}}\right)^2\right)^{\frac{1}{2}} = \frac{1}{2} B_o^2 \ . \qquad (A4)$$

Equation (A4) is analogous to the equation of a particle in a potential
$\varphi(A) = \mu_o N M v_{\perp o}^2 \left[1 - \left(\frac{eA}{M v_{\perp o}}\right)^2\right]^{\frac{1}{2}}$ shown in the solid curve of Fig. 7, where
A is analogous to the particle position and y to time. There are two
types of solution: class 1 where $\frac{B^2}{2\mu_o} > N_o M v_{\perp o}^2$, and class 2 where
$\frac{B^2}{2\mu_o} < N_o M v_{\perp o}^2$. The vector potential and magnetic field are shown
as a function of y in Fig. 8. Notice that class 1 solutions are the
only reasonable solutions for magnetically shielded beam propagation
since the magnetic field does not change sign on crossing the beam.
Also since $B(+\infty) = B(-\infty)$, there is no net ion current in the x direction.
However, class 1 solutions do not completely exclude the field unless
$\frac{B^2}{2\mu_o} = N_o M v_{\perp o}^2$, in which case the zero of B is infinitely far from the
position where $B = B_o$. Notice that the condition for field exclusion
is simply that $v_{\perp o} > V_A$ as stated in Sec. V.

In order for B(y) to go to zero in a finite space the potential
$\varphi(A)$ must have a sharp, rather than smooth, top (discontinuous dA/dy)
as shown by the dashed curve in Fig. 7. Since the electron pressure
is very small compared to the ion pressure, and the electron Larmor
radius is roughly m/M compared to the ion Larmor radius, then the
electron pressure $p_e(A)$ can reasonably be considered to have a sharp
maximum as in Fig. 7.

23

To go back to the description of $A(y)$ via the analogy with particle motion in a potential field, if the particle energy is equal to the maximum potential energy, then the particle comes to rest on top in a finite time. It can then remain at rest for any arbitrary time, and finally roll off the other side. The vector potential and magnetic field corresponding to such a solution of Eq. (A2) is shown in Fig. 9. Notice that there is an arbitrary sized region having $B = 0$ through which the remainder of the beam can propagate.

Finally, we should point out that the nature of the equilibrium we have calculated is independent of the particular form of F_i. As long as $p_i(A)$ has a maximum point somewhere, and $p_e(A)$ has a sharp top at the maximum of $p_i(A)$, such a magnetically shielded equilibrium can form.

ACKNOWLEDGMENT

24
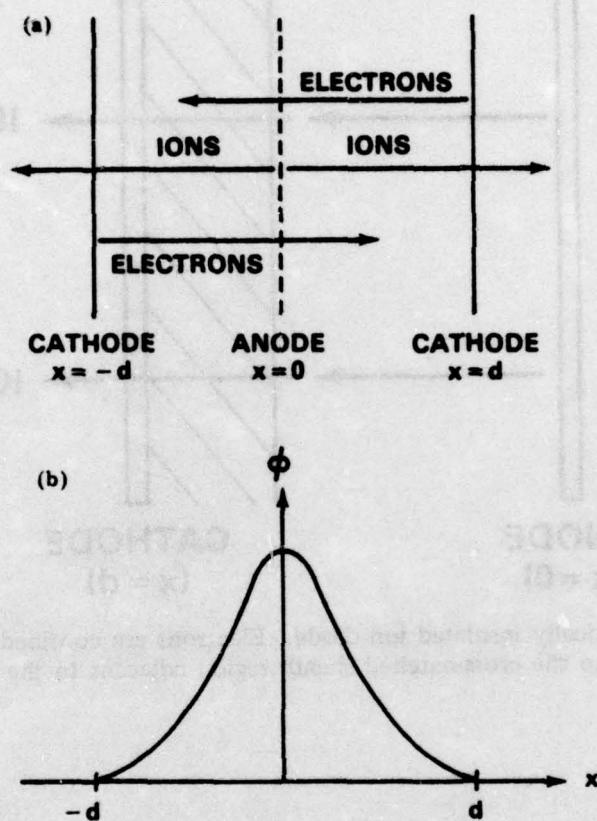
Fig. 1 — Reflex triode: (a) electrode configuration;
(b) electrostatic potential versus x
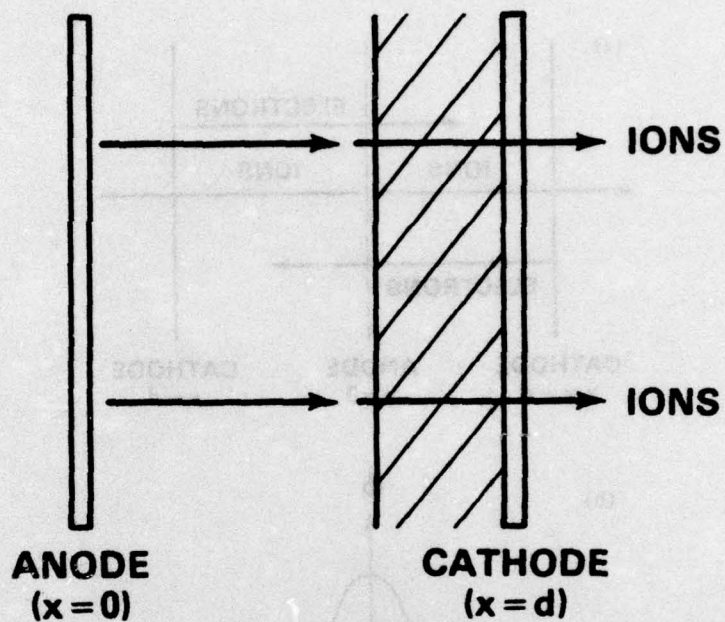
Fig. 2 — Magnetically insulated ion diode. Electrons are confined by the magnetic field to the cross-hatched sheath region adjacent to the cathode
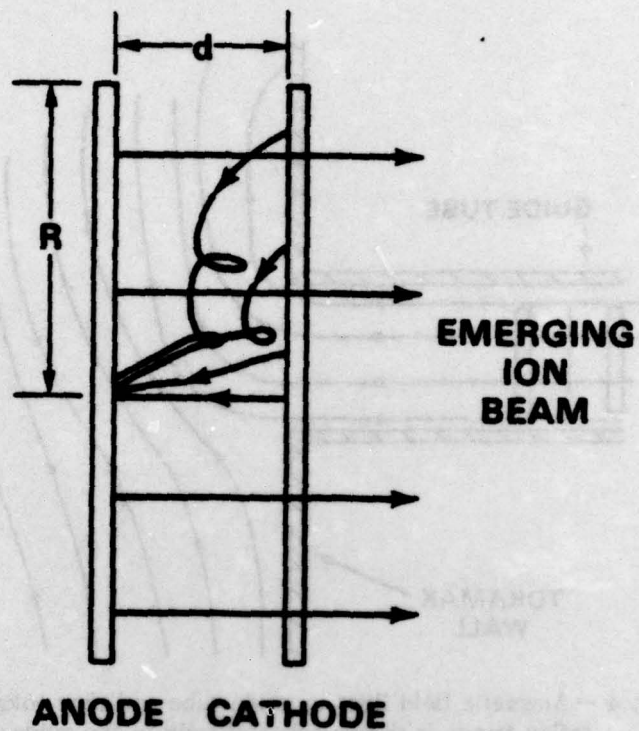
Fig. 3 — Electron pinch diode, showing typical electron orbits in the self-consistent azimuthal magnetic field and typical ion orbits (which are essentially straight)
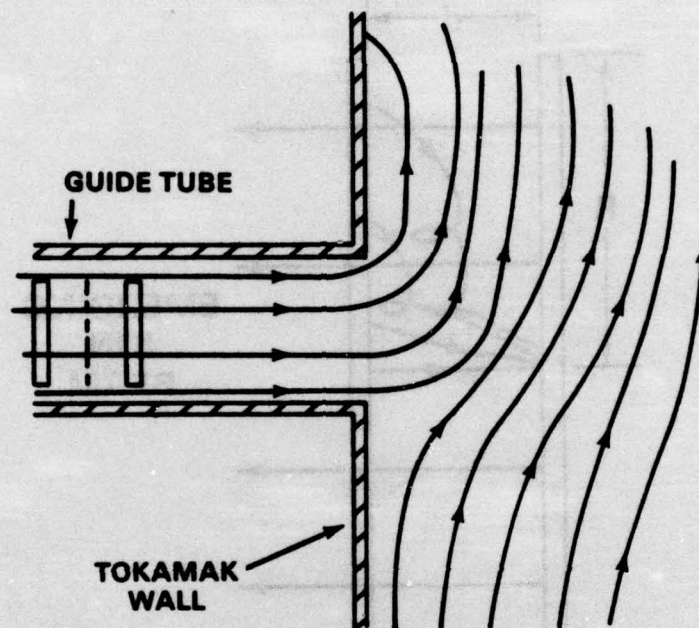
Fig. 4 — Magnetic field lines in guide tube and near tokamak wall.
A reflex triode is shown schematically in the guide tube.
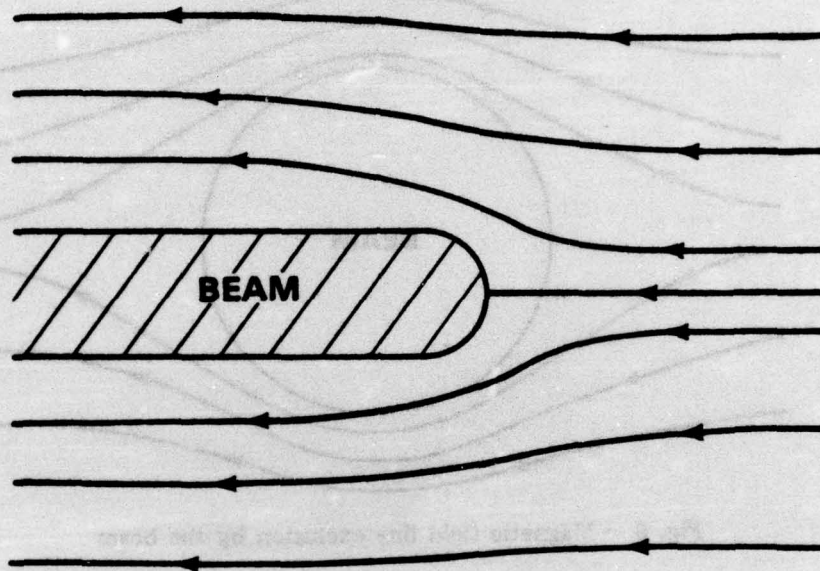
Fig. 5 — Plasma flow around beam on equipotentials in the beam frame
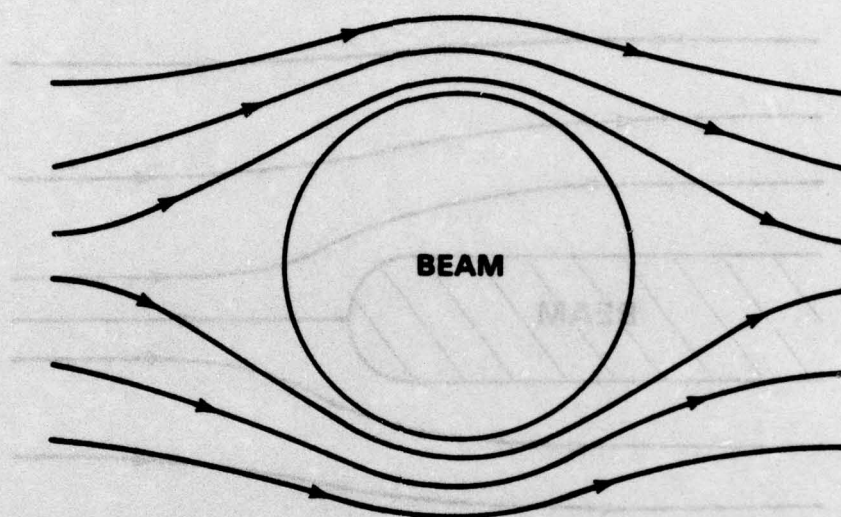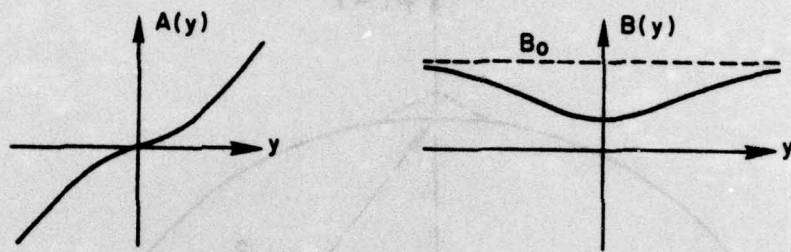
Fig. 6 — Magnetic field line exclusion by the beam
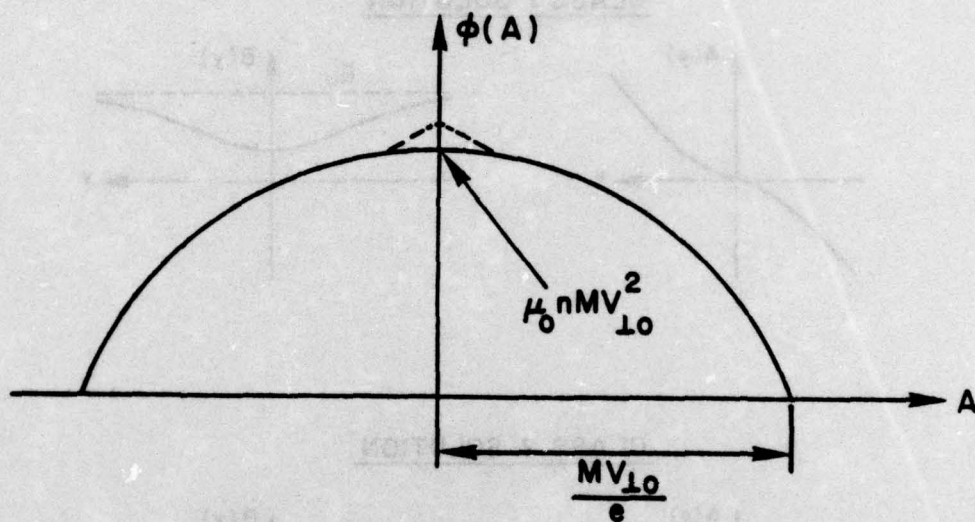
Fig. 7 — $\varphi(A)$ versus A. Solid line is contribution of ions alone. Dashed line illustrates the effect of electrons.

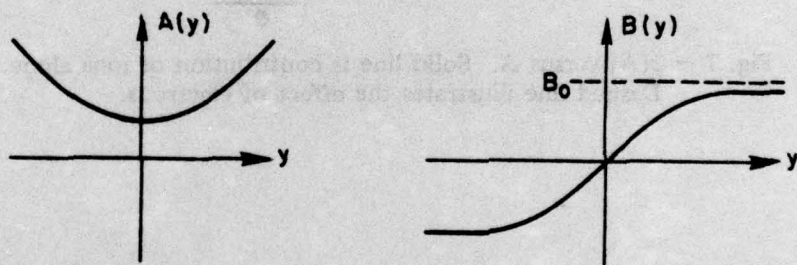**CLASS 1 SOLUTION**

CLASS 2 SOLUTION

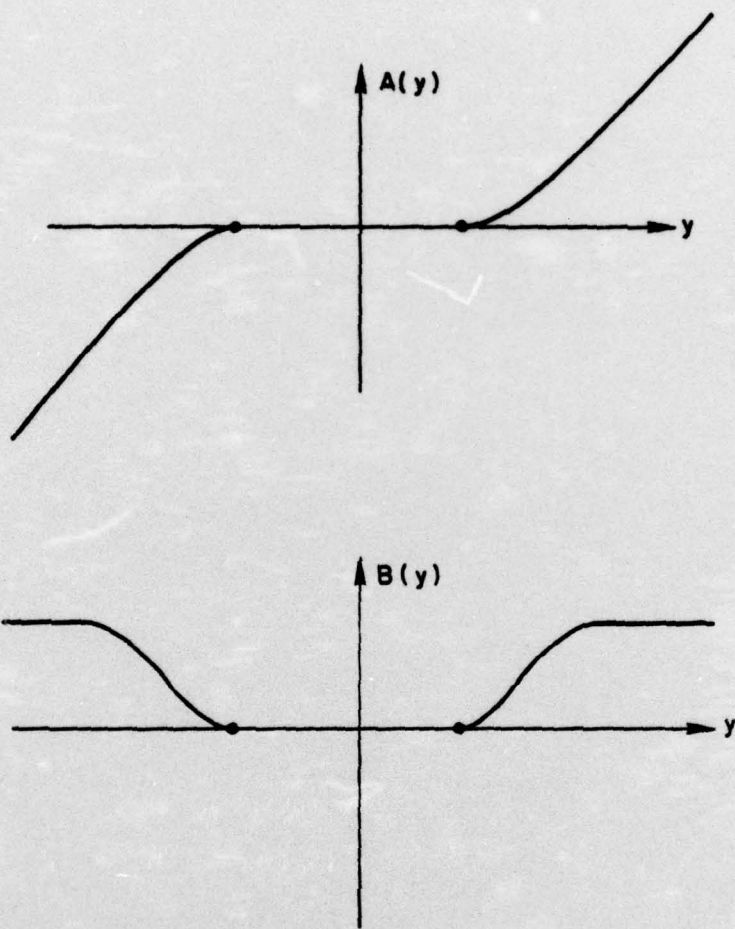Fig. 8 — Two classes of solution for Eq. (A4) (with ion pressure only)

Fig. 9 — Solution with electron pressure included

33